3-D Location System Employing BLE and Frequency-Scanned Antennas

José A. López Pastor[1,*], Antonio D. Hernández Mateos[2], Alejandro Gil Martínez[3], Astrid Algaba Brazález[2] and José L. Gómez Tornero[2]

[1]Department of Information and Telecommunication Technologies, University Center of Defense (CUD), San Javier Air Force Base, MDE-UPCT, Spain

[2] Department of Information and Communication Technologies, Technical University of Cartagena, Cartagena, Spain

[3]Department of Information and Communications Engineering, University of Murcia, Murcia, Spain

Abstract

A novel Bluetooth Low Energy (BLE) 3-D localization system employing frequency-scanned leaky wave antennas (FSLWA) is proposed and evaluated in this work. The system employs the separate-channel fingerprinting (SCFP) technique, which processes the Received Signal Strength Indicator (RSSI) measurements from the different BLE advertising channels independently. FSLWAs are specifically configured to multiplex each BLE advertising channel into a distinct spatial direction. This makes the resulting separate-channel radiomaps spatially more diverse, thus enhancing the localization accuracy compared to conventional monopole-based systems. The proposed system was tested in an indoor environment measuring 7 m x 5m x 2.6 m across five different height levels. The performance of the BLE system connected to FSLWA has been compared against a baseline system using BLE dongles with conventional monopole antennas. Results show that the proposed approach, combining FSLWA with SCFP, achieves a 27.27% improvement in the 3D mean localization error compared to the monopole-based system.

Keywords

Bluetooth Low Energy (BLE), separate-channel fingerprinting, 3D indoor location, frequency-scanned leaky-wave antennas

1. Introduction

The implementation of Indoor Real-Time Location Systems (IRTLS) of IoT devices has become a key enabler in the evolution of Smart Spaces, Industry 5.0, and other emerging technological paradigms. Dynamic environments, like manufacturing plants, logistics hubs, hospitals, and smart buildings, require continuous and accurate tracking of mobile assets, such as people, tools, and equipment. In these scenarios, where collaboration between humans and machines is prioritized, reliable indoor positioning information is fundamental to ensure operational efficiency, safety, and traceability [1].

In this context, several studies in the scientific literature have implemented two-dimensional (2-D) BLE fingerprinting systems [2]. However, real-world IRTLS deployments increasingly demand three-dimensional (3-D) capabilities. This requirement is particularly relevant in multi-floor buildings, vertical warehouses, airports, and healthcare facilities, where assets and individuals frequently move across different elevation levels. In response to this need, multiple 3-D BLE systems have recently been proposed. However, extending BLE-based fingerprinting to three dimensions presents specific challenges due to the limited spatial diversity of RSSI in the vertical axis, especially when employing conventional omnidirectional antennas.

To address this limitation, the present work proposes an extension of our previous 2-D BLE indoor positioning system [3] into a system with 3-D capabilities. The proposed approach is based on separate channel fingerprinting (SCFP) and frequency-scanned leaky-wave antennas (FSLWAs), forming a

IPIN-WCAL 2025: Workshop for Computing & Advanced Localization at the Fifteenth International Conference on Indoor Positioning and Indoor Navigation, September 15–18, 2025, Tampere, Finland

*Corresponding author.

joseantonio.lopez@cud.upct.es (J. A. L. Pastor); adavid.hernandez@edu.upct.es (A. D. H. Mateos); alejandrorafael.gil@um.es (A. G. Martínez); astrid.algaba@upct.es (A. A. Brazález); josel.gomez@ucpt.es (J. L. G. Tornero)

0000-0001-8266-8669 (J. A. L. Pastor)

complete 3-D localization framework. SCFP leverages the BLE advertising channels, which operate at distinct frequencies, each exhibiting different propagation characteristics due to multipath fading and frequency-selective attenuation [4, 5, 6, 7]. In addition, the use of FSLWAs, which radiate each BLE channel in a different spatial direction, further enhances the spatial-frequency diversity by generating distinct and less correlated radiomaps per channel. This "iridescent" or "prism" effect of FSLWAs [8] has already demonstrated application for Angle-of-Arrival localization employing not only BLE networks but also other wireless protocols such as Wi-Fi [9], passive RFID sensor network and also THz networks.

In this paper, we investigate for the first time the application of SCFP with FSLWA antennas in a 3-D indoor positioning context. By incorporating spatial, vertical, and horizontal diversity into the radiomap calibration process, we aim to evaluate the benefits of frequency-scanned antennas for both horizontal positioning and height estimation. The main contributions of this work are:

1. The introduction of a novel SCFP technique was introduced based on RSSI measurements from BLE beacons connected to FSLWAs
2. The analysis of separate-channel radiomaps acquired at different heights using BLE in conjunction with FSLWAs
3. The performance of the proposed SCFP-based 3-D localization system, compared to conventional approaches employing monopole antennas and unified-channel fingerprinting

2. BLE System with FSLWA and test scenario

The employed antenna is a dual-port bi-directionally fed microstrip leaky-wave antenna designed to steer the three BLE advertising channels in different spatial directions. A commercial BLE dongle, acting as a receiver, is connected to each port (P1 and P2), as illustrated in Fig.1a. For comparison, the traditional BLE system is illustrated in Fig.1b, consisting of a monopole antenna connected to a single-port BLE dongle. The radiation patterns of both the FSLWA and the monopole were measured in an anechoic chamber using a rotating platform, with measurements conducted across the three advertising channels. Fig.1c displays the radiation patterns of the FSLWA for channel #37 (red), channel #38 (green), and channel #39 (blue). As observed, six distinct beams are obtained, pointing at different angles depending on the channel frequency, increasing the pointing angle with frequency. In contrast, as shown in Fig.1d, the monopole antenna exhibits a frequency-independent radiation pattern, maintaining uniform angular coverage from -60° to +60°.

The experimental setup was deployed in a 7-meter by 5-meter room with a ceiling height of 2.65 meters, as depicted in the photograph in Fig.2a and the schematic diagram in Fig.2b. A total of 650 test points were uniformly distributed across five height levels, with 130 points per height. The vertical spacing between height levels was 50 cm, starting at 0 cm (i.e., directly on the floor) and extending up to 200 cm above the floor. Horizontally, the test points formed a uniform grid with 50 cm spacing between neighboring points. The room's ceiling includes a metallic grid structure, which contributes to a rich multipath propagation environment. Two separate setups were created to enable a fair comparison between the FSLWA and monopole-based systems. The first configuration employs four BLE dongles interfaced with two FSLWAs, where P1 and P2 dongles correspond to LWA1, and P3 and P4 to LWA2. The second configuration consists of four commercial BLE dongles, each equipped with a monopole antenna, denoted as P5, P6, P7, and P8 as observed in Fig.2b

The eight BLE dongles from both subsystems operate as receivers. An additional BLE dongle, equipped with a monopole antenna, serves as a transmitter and was sequentially placed at each of the 650 test points across the five height levels. All eight receiver dongles were connected to a single personal computer (PC) via a USB hub. At the same time, the transmitting beacon was also connected to the same PC through a separate USB interface. This configuration allowed synchronized data acquisition across all eight receivers, ensuring measurement consistency and enabling a fair and direct comparison of localization performance between the two systems.

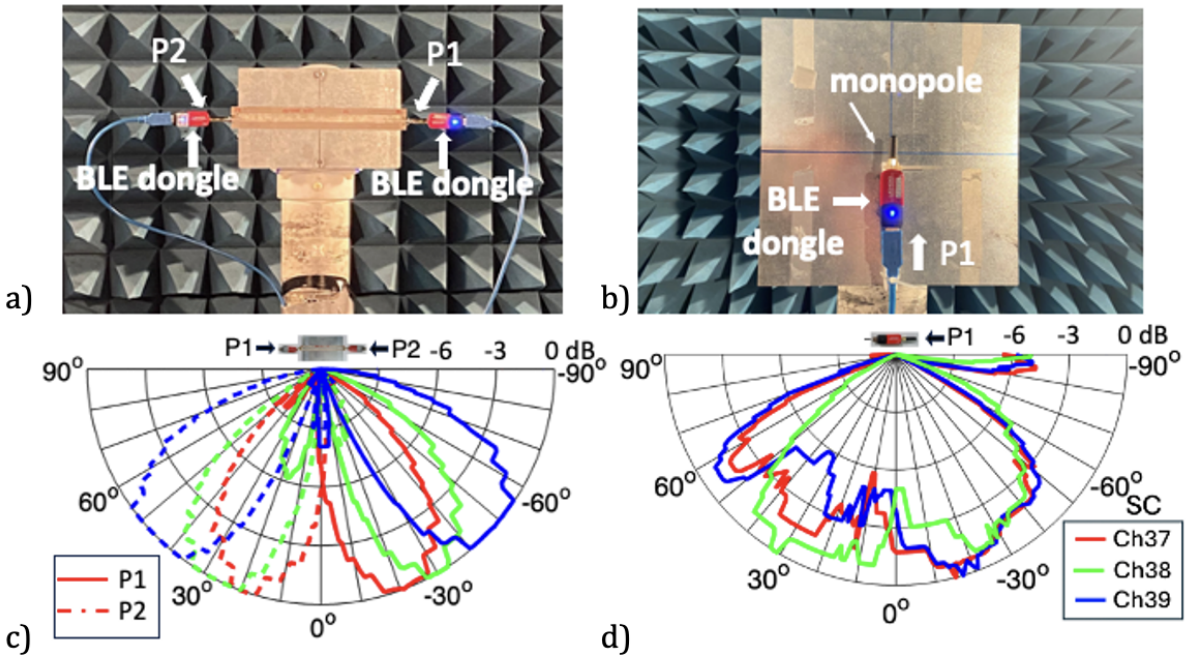

Figure 1: a) FSLWA with two BLE dongles connected to the two ports (P1 and P2). b) Monopole with a single BLE dongle connected to its single port (P1). c) Measured radiation pattern of the three advertising channels in the FSLWA measured at anechoic chamber d) Radiation pattern of the monopole.

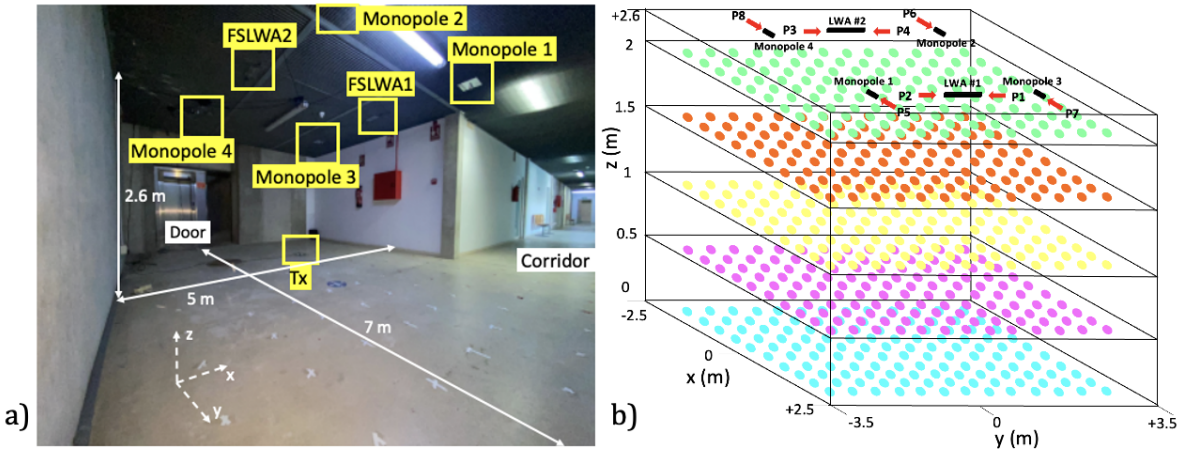

Figure 2: a) Picture of the test scenario with the set-up dimensions. b) 3-D diagram with the position of the different test points and the distribution of monopoles and FSLWAs.

2.1. Measured radiomaps

The SCFP technique is based on generating a set of calibrated radiomaps with the RSSI, each corresponding to a distinct BLE advertising channel. As previously mentioned, the monopole antenna and FSLWA systems are positioned at fixed locations to ensure comprehensive and consistent radiomap coverage. Following this set-up, RSSI measurements were conducted to examine the propagation differences between the two antenna types. The measured radiomaps are plotted in Fig.3. For illustrative purposes, we have chosen to display only the radiomaps corresponding to two ports of one FSLWA and one monopole antenna, as these are considered sufficiently representative of the observed propagation behavior. Fig.3a, b, and c illustrate the measured radiomaps from LWA1 and port P1 for channels #37, #38, and #39, respectively. Fig. 3d, e, and f correspond to measurements from LWA1 and P2 for channels #37, #38, and #39. Finally, Fig. 3g, h, and i display the radiomaps obtained for Monopole 3 and channels #37, #38, and #39. The five measurement heights are represented as horizontal slices, and the -30 dB

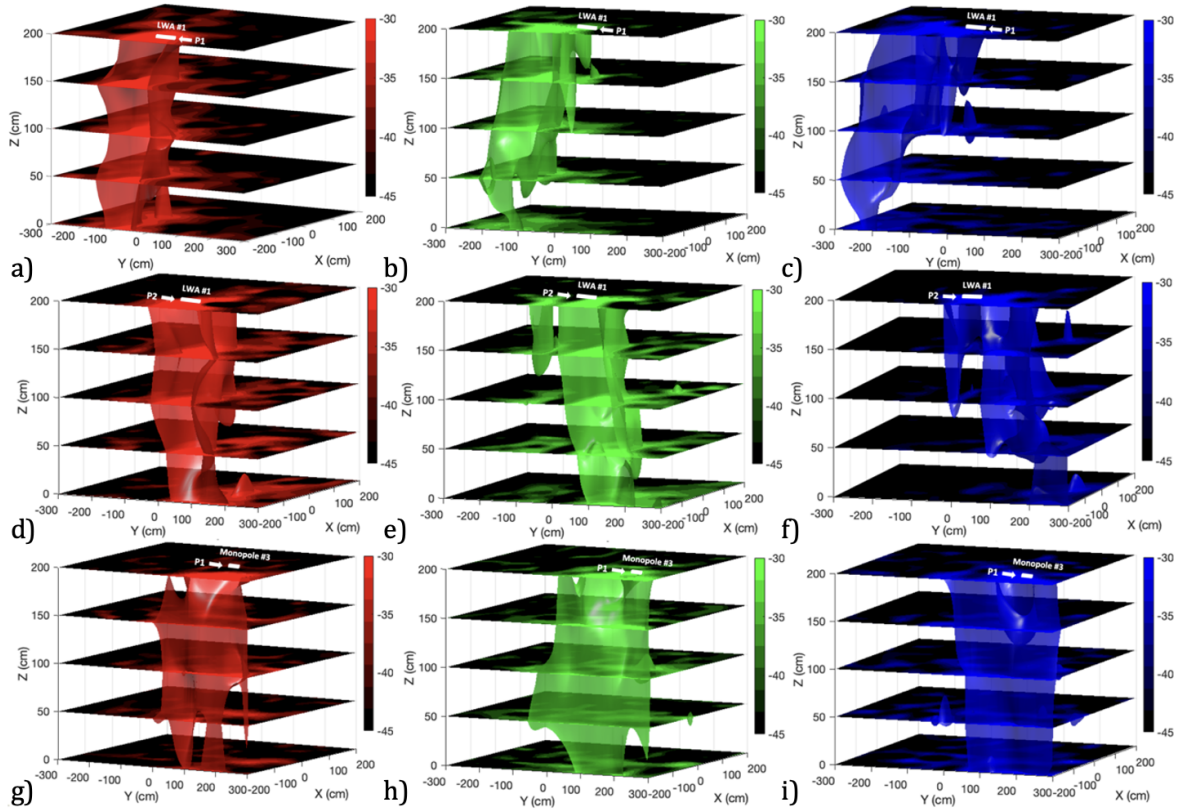

Figure 3: Measured RSSI at different heights and representation of the propagation effects for a) LWA1 P1 #37; b) LWA1 P1 #38; c) LWA1 P1 #39; d) LWA1 P2 #37; e) LWA1 P2 #38; f) LWA1 P1 #39; g) Monopole3 #37; h) Monopole3 #38; i) Monopole3 #39.

signal level has been visualized by joining these slices as a continuous surface, creating a volumetric impression of signal distribution. As observed, the "illuminated" region produced by the FSLWA varies significantly across the measured channels, confirming the frequency-scanning behavior of the FSLWA. The strongest radiation zone for the lowest frequency (channel #37, shown in red color) appears nearly perpendicular for both ports, pointing below the antenna's position. As the frequency increases (e.g., channel #38 in green), the beam shifts to a wider angle. Finally, for the highest frequency (channel #39 in blue), the beam points toward the edge of the room. In contrast, the monopole antenna exhibits a stable radiation pattern across all three channels, consistently directing energy below the antenna, regardless of the operating frequency.

As discussed in the following section, this frequency-dependent variability in RSSI distribution for the FSLWA results in richer, more spatially diverse radiomaps, ultimately leading to enhanced accuracy in fingerprint-based localization.

3. Fingerprint Localization Results

In this section, we describe the fingerprint process employed and compare the results obtained from the two different subsystems: one using the FSLWA and the other using monopole antennas. The fingerprinting procedure involves a calibration stage, during which initial radiomaps are acquired and stored in a database. Each radiomap consists of a set of vectors, where each vector contains the RSSI values measured at a specific reference point from all BLE beacons. In our setup, two distinct calibration radiomaps are generated: one from the FSLWA-based system and the other from the monopole-based system. Each radiomap comprises 650 calibration vectors, corresponding to the 650 test points. In both systems, each vector contains 12 RSSI values, three from each of the four BLE dongles (one per advertising channel).

During the localization stage, an RSSI sample is acquired at an unknown position. This sample, structured as a test vector containing RSSI values from the three advertising channels of each beacon, is then compared with the stored calibration radiomap. Several methods can be used to compute similarity between the test and calibration vectors, including correlation analysis, machine learning algorithms, or deep learning techniques. In this work, we use a simple correlation method implemented using the "`corrcoef`" function in MATLAB, to evaluate the similarity between the test vector and the reference vectors in the radiomap.

3.1. Data generation

In this case, the data acquisition process was not as complete as desired. The main limitation is that only 10 RSSI samples were collected at each of the 650 reference points. Consequently, the dataset does not contain enough samples to generate both a calibration radiomap and an independent subset for test vector generation. To address this limitation, we used our previously published open dataset [10, 11], to generate artificial test samples. This dataset includes calibration and test data collected over multiple days, up to the 96th day after the initial calibration, although it is limited to floor-level measurements. To synthesize the artificial RSSI test data, we first computed the standard deviation at each reference point using all the data available in the repository [10, 11]. Since propagation characteristics vary depending on the advertising channel and the antenna used, we calculated the standard deviation for each point individually, taking into account each port and advertising channel combination. Specifically, we computed distinct standard deviation matrices for all 130 reference points, one for each BLE port and advertising channel. We denote these matrices as $M\boldsymbol{\sigma}_{i,j}\mathrm{PX}\#Y$, where *i,j* are the coordinates of the 130 test points, PX denotes the different BLE ports from 1 to 8, and #Y refers to the BLE advertising channels #37, #38, and #39. In total, we generated 24 standard deviation matrices (8 ports × 3 channels), each containing 130 values corresponding to the different reference points, based on the samples from dataset [10, 11].

Once the standard deviation matrices were computed, they were used to generate noisy samples based on the 10 original RSSI measurements collected at each of the 650 reference points. We have generated four subsets of samples by employing a random value between [-1,1] × $\boldsymbol{\sigma}_{i,jPX\#Y}$, [-2, 2] × $\boldsymbol{\sigma}_{i,jPX\#Y}$,[-3,3] × $\boldsymbol{\sigma}_{i,jPX\#Y}$, and [-4,4] × $\boldsymbol{\sigma}_{i,jPX\#Y}$. Therefore, we now have four subsets of samples. The greater the noise and standard deviation values, the greater the uncertainty in the prediction. For each of the 10 samples, we generated an additional 10 samples using the standard deviation and bounded random noise. Therefore, each of the 650 test points now contains 100 test samples per dataset, enabling the evaluation of the system's robustness under increasing uncertainty.

3.2. Accuracy and spatial distribution of the correlation function

Using the previously generated test matrices, we computed the correlation between each test vector and the calibrated radiomaps to estimate a 3-D position. The localization error was then calculated as the Euclidean distance between the estimated point and the actual reference point where the sample was acquired. Table I presents the mean localization error in cm for different noise levels, comparing the system based on FSLWAs and the system using monopole antennas. As observed, the improvement in accuracy employing FSLWA when the random RSSI noise is [-1,1] × $\boldsymbol{\sigma}_{i,jPX\#Y}$ results to be 27.27%, and still a 5.82% improvement is achieved when the random RSSI noise is [-4,4] × $\boldsymbol{\sigma}_{i,jPX\#Y}$.

Additionally, we analyzed the spatial distribution of the correlation function (SDCF) when a test vector is compared with the calibration radiomap. This SDCF reaches a maximum value of 1 in the coordinate x, y, z when the value is perfectly correlated. This value decreases from 1 to 0 as the vectors become less correlated. Fig.4 illustrates the SDCF regions for a confidence level of 0.95 (yellow color) and 0.90 (blue color), for the system using FSLWAs (Fig.4a) and the system employing monopoles (Fig.4b). The real point where the measurement was acquired is marked with an (*), and the estimated point by the correlation is indicated with a red dot. In both cases, the evaluated test position is 75, 75, 100. As observed, the estimated location is properly determined by both systems. However, it can be

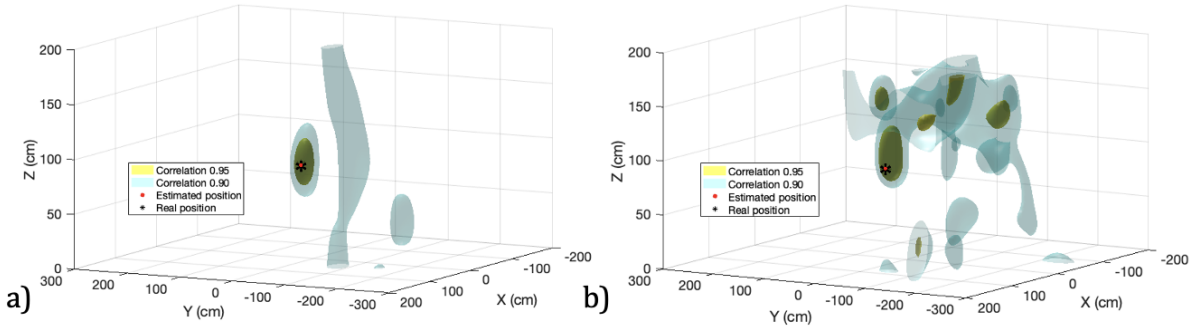

Figure 4: a) 3-D spatial distribution of the correlation function (SDCF) in a specific point for a) FSLWA system; b) Monopole system

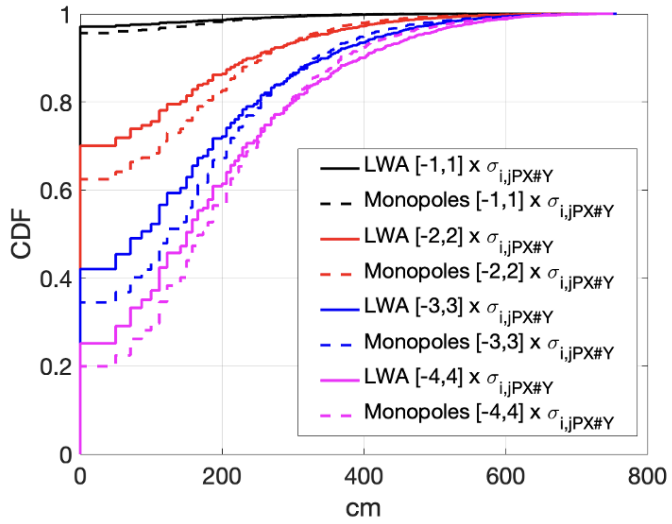

Figure 5: a) 3-D spatial distribution of the correlation function (SDCF) in a specific point for a) FSLWA system; b) Monopole system

observed that the 0.95 confidence interval is more compact and better defined for the FSLWA-based system. In contrast, the 0.95 confidence interval for the monopole-based system exhibits multiple regions, indicating a broader spatial area with high correlation values. Similar behavior is observed for the 0.90 confidence level, where the monopole system also displays extended regions of uncertainty. This example highlights that the FSLWA-based system provides more spatial precision, as it produces smaller, more localized correlation zones. Consequently, the Cumulative Distribution Function (CDF) of the localization error for both systems, as shown in Fig. 5, reveals that the FSLWA system consistently outperforms the monopole-based system. Regardless of the level of RSSI noise applied, the FSLWA system achieves higher localization accuracy across the entire range of error distributions.

4. Conclusions

In this paper, we present a novel 3-D indoor localization framework that combines Separate-Channel Fingerprinting (SCFP) of BLE advertising channels with Frequency-Scanned Leaky-Wave Antennas (FSLWAs). The “iridescent” effect of the FSLWA leads to separate channel fingerprint patterns that are less correlated across height levels, addressing one of the key limitations of conventional monopole-based BLE systems. Extensive experiments in a 7 m × 5 m × 2.65 m room, covering 650 uniformly distributed test points at five heights, demonstrate the accuracy of the proposed approach. Under baseline noise conditions (±1 σ), the FSLWA-based system achieves a mean 3-D localization error of 5.97 cm, representing a 27.27% improvement over the monopole-based baseline (8.22 cm). Even under

Table 1
Error for the different BLE/Monopole systems and different noise applied

	Mean error (cm)	Mean Improve LWA vs Monopole
[-1,1] × $\boldsymbol{\sigma}_{i,jPX\#Y}$	5.97	27.27%
[-2,2] × $\boldsymbol{\sigma}_{i,jPX\#Y}$	63.6	18.16%
[-3,3] × $\boldsymbol{\sigma}_{i,jPX\#Y}$	128.17	10.37%
[-4,5] × $\boldsymbol{\sigma}_{i,jPX\#Y}$	173.19	5.82%
[-1,1] × $\boldsymbol{\sigma}_{i,jPX\#Y}$	8.22	
[-2,2] × $\boldsymbol{\sigma}_{i,jPX\#Y}$	77.35	
[-3,3] × $\boldsymbol{\sigma}_{i,jPX\#Y}$	143.01	
[-4,5] × $\boldsymbol{\sigma}_{i,jPX\#Y}$	184.32	

elevated noise levels (up to ±4 $\boldsymbol{\sigma}$), the FSLWA configuration consistently outperforms the monopole setup, with performance gains of 18.16%, 10.37%, and 5.82%for noise bounds of ±2$\boldsymbol{\sigma}$, ±3 $\boldsymbol{\sigma}$, and ±4 $\boldsymbol{\sigma}$, respectively. Future work will focus on optimizing antenna design and placement for even greater spatial resolution, integrating mobile nodes (e.g., drones or handheld devices), and evaluating performance in dynamic and cluttered scenarios, further assessing robustness and scalability.

Acknowledgments

This work was supported by the Spanish National project TED2021-129196BC42, PID2022-136590OB-C42, and REPNIN++ RED2022-134355-T. The work of A. Algaba-Brazález is supported by the Grant RYC2022-037385-I funded by MCIN/AEI /10.13039/501100011033 and by "ESF Investing in your future".

Declaration on Generative AI

The author(s) have not employed any Generative AI tools.

References

[1] F. J. Aranda, F. Parralejo, F. J. Álvarez, J. A. Paredes, Performance analysis of fingerprinting indoor positioning methods with ble, Expert Systems with Applications 202 (2022) 117095. URL: https://www.sciencedirect.com/science/article/pii/S0957417422005012. doi:https://doi.org/10.1016/j.eswa.2022.117095.

[2] F. J. Aranda, F. Parralejo, T. Aguilera, F. J. Álvarez, J. Torres-Sospedra, Finding optimal ble configuration for indoor positioning with consumption restrictions, in: 2021 International Conference on Indoor Positioning and Indoor Navigation (IPIN), 2021, pp. 1–8. doi:10.1109/IPIN51156.2021.9662563.

[3] J. López-Pastor, A. Gil-Martinez, A. Hernández-Mateos, A. Algaba-Brazález, J. Gómez Tornero, Bluetooth low energy separate-channel fingerprinting with frequency-scanned antennas, Elsevier Internet of Things in press (2025).

[4] G. De Blasio, A. Quesada-Arencibia, C. R. García, J. C. Rodríguez-Rodríguez, R. Moreno-Díaz, A protocol-channel-based indoor positioning performance study for bluetooth low energy, IEEE Access 6 (2018) 33440–33450. doi:10.1109/ACCESS.2018.2837497.

[5] M. Nikodem, P. Szeliński, Channel diversity for indoor localization using bluetooth low energy and extended advertisements, IEEE Access 9 (2021) 169261–169269. doi:10.1109/ACCESS.2021.3137849.

[6] S. Ishida, Y. Takashima, S. Tagashira, A. Fukuda, Design and Initial Evaluation of Bluetooth Low

Energy Separate Channel Fingerprinting, Springer International Publishing, Cham, 2018, pp. 19–33. URL: https://doi.org/10.1007/978-3-319-70636-8_2. doi:10.1007/978-3-319-70636-8_2.

[7] V. Cantón Paterna, A. Calveras Augé, J. Paradells Aspas, M. A. Pérez Bullones, A bluetooth low energy indoor positioning system with channel diversity, weighted trilateration and kalman filtering, Sensors 17 (2017). URL: https://www.mdpi.com/1424-8220/17/12/2927. doi:10.3390/s17122927.

[8] B. Zhai, Y. Zhu, A. Tang, X. Wang, Thzprism: Frequency-based beam spreading for terahertz communication systems, IEEE Wireless Communications Letters 9 (2020) 897–900. doi:10.1109/LWC.2020.2974468.

[9] J. A. López-Pastor, M. Poveda-García, A. Gil-Martínez, D. Cañete-Rebenaque, J. L. Gómez-Tornero, 2-d localization system for mobile iot devices using a single wi-fi access point with a passive frequency-scanned antenna, IEEE Internet of Things Journal 10 (2023) 14995–15011. doi:10.1109/JIOT.2023.3262830.

[10] J. López-Pastor, A. Gil-Martinez, A. Hernández-Mateos, A. Algaba-Brazález, J. Gómez Tornero, Bluetooth low energy dataset using separate-channel fingerprinting techniques and frequency scanned antennas, Scientific Data 12 (2025) 255. URL: https://doi.org/10.1038/s41597-025-04581-0. doi:10.1038/s41597-025-04581-0.

[11] J. A. López-Pastor, A. D. Hernández-Mateos, A. Gil-Martínez, A. Algaba-Brazález, J. L. Gomez-Tornero, Bluetooth low energy separate channel fingerprinting dataset with frequency-scanned antennas and monopole, 2024. doi:10.5281/ZENODO.10721782.